

Interference in a system of coupled quantum wires: Theoretical study of electronic transport

Bogdan R. Buřka,¹ Mugurel Ţolea,² and Ion V. Dinu^{1,2}

¹*Institute of Molecular Physics, Polish Academy of Sciences, ul. M. Smoluchowskiego 17, 60-179, Poznań, Poland*

²*National Institute of Materials Physics, P.O. Box MG7, Bucharest-Magurele, Romania*

(Received 21 July 2006; published 1 November 2006)

Theoretical studies of the coherent electronic transport in a system of coupled quantum wires show that switching on the conducting channel in one wire can be manifested in the other coupled wires. Interference processes and electronic correlations are taken into account in our studies on the same footing. The conductance changes depend on the interference conditions of a transmitted wave with that one reflected from the wires that indirectly influence the transport. We show that electronic correlations lead to a dynamical Coulomb blockade effect, which changes the conductance response quantitatively but its shape is still kept the same. Our results are discussed in correspondence with an experiment recently performed by Morimoto *et al.* [Appl. Phys. Lett. **82**, 3952 (2003)] on a system of coupled quantum wires.

DOI: [10.1103/PhysRevB.74.205301](https://doi.org/10.1103/PhysRevB.74.205301)

PACS number(s): 73.23.-b, 73.63.Rt, 85.35.Ds, 85.35.Be

I. INTRODUCTION

The system of coupled quantum wires has attracted interest for its potential applications in electronic devices¹—for example, as quantum logic gates^{2,3} in quantum computers. Operation of the device is based on coherent coupling of electronic waves propagating through the quantum wires. In the first experiments¹ the tunnel coupling between two waveguides was rather weak, but observable. The tunneling currents increase when a new mode begins to propagate through the wire. Recently, Morimoto *et al.*⁴ studied the transport in a system of quantum wires coupled through a quantum dot [see Figs. 1(a) and 1(b)]. They measured the conductance \mathcal{G}_{up} in the upper wire [Fig. 1(a)] as a function of the gate voltage V_g , which controls the current flowing in the lower wire [Fig. 1(b)]. For low voltages, when the current in the lower wire is blocked, the swept voltage had little influence on \mathcal{G}_{up} . However, for a higher V_g , when the first mode became propagated in the lower wire and the conductance \mathcal{G}_{low} formed its first step, a resonant peak was observed in \mathcal{G}_{up} . Puller *et al.*⁵ explained this effect as a tunnel-induced correlation, which arises from the interaction between a localized magnetic moment with both channels.

The purpose of our work is to show the role of interference processes between electronic waves propagating in both channels, which can modify the electronic transport in the upper wire when electrons are allowed to flow through the lower wire. If the lower wire is switched off (for a high V_g), the upper wire is coupled only to the quantum dot (QD). In this case one can expect the Fano resonance, which can lead to destructive interference and lowering the conductance \mathcal{G}_{up} .⁶ The shape of the conductance depends on the Fano parameter q , and \mathcal{G}_{up} can have a large peak, but a dip always appears, which manifests destructive interference. Electronic correlations on the QD lead to Kondo resonance. The conductance in high temperatures has two dips, separated by charging energy U , which merge into one broad dip in low temperatures.⁷ Recent experiments performed by Sato *et al.*⁸ gave evidence for the Fano-Kondo resonance in such systems.

II. RESONANT TRANSMISSION

The model corresponding to the experimental situation studied by Morimoto *et al.*⁴ is presented in Fig. 1(c). This is a three-terminal system, in which the current J_{up} flowing from the left to the right electrode corresponds to the situation in Fig. 1(a) and the current J_{low} flowing from the right to the central electrode corresponds to the situation in Fig. 1(b). We want to study the dependence on both the currents on the gate voltage eV_g , which switches on the central electrode.

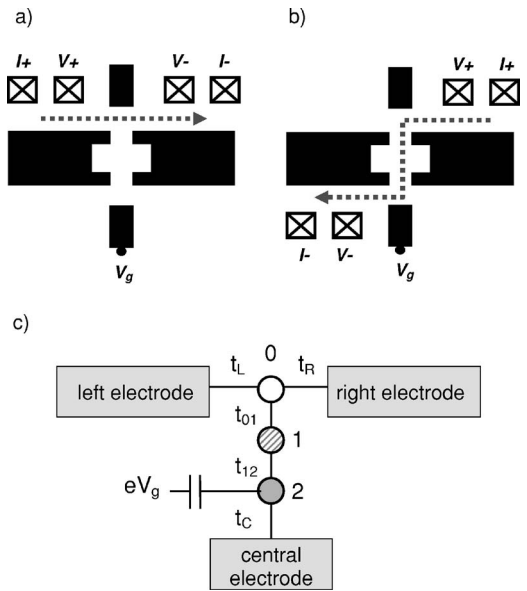


FIG. 1. Schematic illustration of the split-gate device studied in Ref. 4. The black regions in the figures represent metal gates, which were deposited on the surface of a GaAs/AlGaAs quantum well. Measurements of the conductance were performed through the upper wire (a) and from the right part of the upper wire, through the quantum dot, to the lower wire (b) as a function of the gate voltage V_g . The voltage in the other electrodes was kept constant. (c) presents the corresponding model, where the left, the right, and the central electrodes are assumed as a reservoir connected to the site “0” or “2,” respectively. The quantum dot is denoted as “1,” and the gate potential shifts the position of the site level “2.”

The Hamiltonian for this model is expressed as

$$\begin{aligned}
 H = & \sum_{k,\sigma,\alpha \in L,R,C} \epsilon_k c_{k\alpha,\sigma}^\dagger c_{k\alpha,\sigma} + \sum_{i=0,1,2,\sigma} \epsilon_i c_{i,\sigma}^\dagger c_{i,\sigma} \\
 & + \sum_{\sigma} (t_{01} c_{0,\sigma}^\dagger c_{1,\sigma} + t_{12} c_{1,\sigma}^\dagger c_{2,\sigma} + \text{H.c.}) \\
 & + \sum_{k,\sigma} (t_L c_{0,\sigma}^\dagger c_{kL,\sigma} + t_R c_{0,\sigma}^\dagger c_{kR,\sigma} + t_C c_{2,\sigma}^\dagger c_{kC,\sigma} + \text{H.c.}).
 \end{aligned} \quad (1)$$

The first term describes electrons in the left, the right, and the central electrodes ($\alpha=L,R,C$); the second and third terms correspond to electrons in the junctions connecting the upper electrodes and the central electrode. We assume that the junctions are represented by single states with site energy ϵ_i and the position ϵ_2 is shifted by the gate potential V_g (i.e., $\epsilon_2=eV_g$). The last term in Eq. (1) is the coupling of the electrodes with the junctions. The current flowing from the α electrode can be derived as⁹

$$J_\alpha = \frac{2e}{h} \int_{-\infty}^{\infty} d\omega 2i\Gamma_\alpha \{f_\alpha(\omega) [G_{i,i}^a(\omega) - G_{i,i}^r(\omega)] - G_{i,i}^<(\omega)\}, \quad (2)$$

where f_α is the Fermi distribution function in the α electrode, the coupling between the α electrode and the i site is given by $\Gamma_\alpha = \pi \rho_\alpha^2 \rho$, and the density of states in the electrodes is taken as constant. $G_{i,i}^{a,r,<}$ denote the advanced, retarded, and lesser Green functions at the sites $i=0$ and $i=2$, respectively. The considered system is three-terminal and, therefore, we follow the procedure proposed for this situation.¹⁰ The current is assumed to be equal zero in the dead wire—i.e., in the central wire $J_C=0$ for the case in Fig. 1(a) and in the left wire $J_L=0$ for the case in Fig. 1(b). Using this condition one can eliminate the lesser Green functions in Eq. (2) and find the potential V_α in the dead wire ($\alpha=C,L$).

For the system without electron-electron interactions the conductance in the upper wire [from the left to the right upper wire, which corresponds the situation in Fig. 1(a)] and from the central to the right upper wire [corresponding to the case in Fig. 1(b)] can be expressed as

$$\mathcal{G}_{up} = \frac{2e^2}{h} \int_{-\infty}^{\infty} d\omega \left(-\frac{\partial f}{\partial \omega} \right) \frac{4\Gamma_L \Gamma_R}{\Gamma_L + \Gamma_R} \text{Im}[G_{0,0}^a(\omega)], \quad (3)$$

$$\mathcal{G}_{low} = \frac{2e^2}{h} \int_{-\infty}^{\infty} d\omega \left(-\frac{\partial f}{\partial \omega} \right) \frac{4\Gamma_R \Gamma_{0C}}{\Gamma_R + \Gamma_{0C}} \text{Im}[G_{0,0}^a(\omega)], \quad (4)$$

where f is the Fermi distribution function at equilibrium, $\Gamma_{0C} = \Gamma_C t_{01}^2 t_{12}^2 / |(\omega - \epsilon_1)(\omega - \epsilon_2 - i\Gamma_C) - t_{12}^2|^2$ is an effective coupling of the 0 site with the C electrode. The retarded Green function $G_{0,0}^r$ is given by

$$G_{0,0}^r = \frac{1}{\omega - \epsilon_0 + i(\Gamma_R + \Gamma_L) - \frac{t_{01}^2}{\omega - \epsilon_1 - \frac{t_{12}^2}{\omega - \epsilon_2 + i\Gamma_C}}}. \quad (5)$$

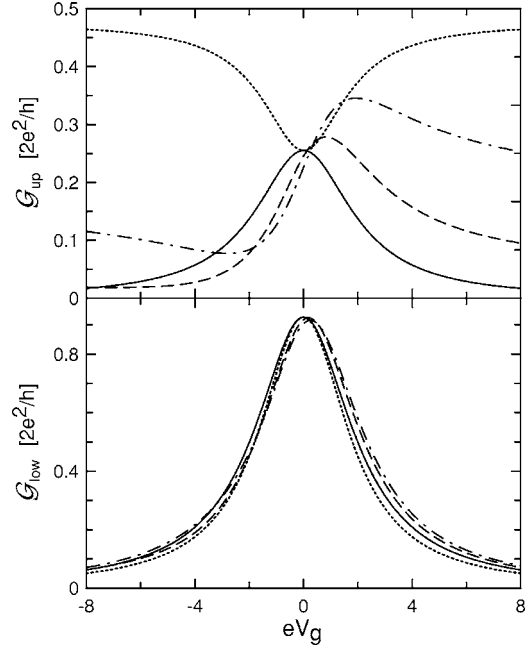


FIG. 2. The conductance \mathcal{G}_{up} in the upper wire (top figure) and \mathcal{G}_{low} from the lower wire (bottom figure) as a function of the gate voltage V_g , which shifts downwards the atomic position $\epsilon_2=eV_g$ for various Fermi energy $E_F=0$ (solid curves), $E_F=-0.25$ (dashed curves), $E_F=-0.5$ (dash-dotted curves), and $E_F=-1.0$ (dotted curves). For positive values of E_F the curves \mathcal{G}_{up} are mirror plots with respect to $eV_g=0$. The other parameters are $\Gamma_L=0.16$, $\Gamma_R=\Gamma_C=1$, $t_{01}=t_{12}=1$, $\epsilon_1=\epsilon_0=0$, and the temperature $T=0$.

The conductance $\mathcal{G}_{up}=\partial J_{up}/\partial V$ in the upper wire and $\mathcal{G}_{low}=\partial J_{low}/\partial V$ in the lower wire are calculated in the limit $V\rightarrow 0$. The results are plotted in Fig. 2 as a function of the applied gate voltage eV_g , which shifts the position of the resonant transmission. The plotted curves are for different Fermi energies E_F . It is seen that \mathcal{G}_{low} is weakly dependent on E_F , while \mathcal{G}_{up} has different shapes. It demonstrates the role of quantum interference of electronic waves penetrating the system. Depending on the phase shift of the penetrating wave, \mathcal{G}_{up} has a different shape, which can be either a symmetric peak (for $E_F=0$), an asymmetric peak with a dip (for $E_F=-0.25, -0.5$), or a symmetric dip (for $E_F=-1$). This is typical situation for Fano resonance.^{6,11} We also calculated \mathcal{G}_{up} for a symmetric coupling, $\Gamma_L=\Gamma_R$, for which the maximal value was obtained smaller than the conductance quantum $2e^2/h$ —as expected for the three-terminal device, where the dead wire plays the role of an inelastic scatterer.¹⁰

III. ELECTRONIC CORRELATIONS IN TRANSPORT

Now, we want to consider electronic interactions and their influence on transport. Therefore, we add to the Hamiltonian (1) the term

$$H_1 = U n_{1\uparrow} n_{1\downarrow}, \quad (6)$$

which describes the Coulomb interactions of electrons with opposite spins at the QD. We can still use the formula (3) for the conductance \mathcal{G}_{up} , which is exact also for the case with interactions.

Determination of the conductance \mathcal{G}_{low} is more complex. First, using Eq. (1) we express the currents J_C flowing out from the central electrode in the form

$$J_C = \frac{2e}{h} \int_{-\infty}^{\infty} d\omega 2i\Gamma_{1C} \{f_{1C}(\omega)[G_{1,1}^a(\omega) - G_{1,1}^r(\omega)] - G_{1,1}^<(\omega)\}. \quad (7)$$

Similarly, the currents J_L and J_R are expressed by the local Green functions $G_{1,1}^{a,r}$ and $G_{1,1}^<$. Since the total current flowing into site "1" $J_L + J_R + J_C = 0$, one can find

$$G_{1,1}^< = \frac{\Gamma_{1L}f_L + \Gamma_{1R}f_R + \Gamma_{1C}f_C}{\Gamma_{1L} + \Gamma_{1R} + \Gamma_{1C}} (G_{1,1}^a - G_{1,1}^r), \quad (8)$$

where $\Gamma_{1L} = \Gamma_L t_{01}^2 / |\omega - \epsilon_0 - i(\Gamma_L + \Gamma_R)|^2$, $\Gamma_{1R} = \Gamma_R t_{01}^2 / |\omega - \epsilon_0 - i(\Gamma_L + \Gamma_R)|^2$, and $\Gamma_{1C} = \Gamma_C t_{12}^2 / |\omega - \epsilon_2 - i\Gamma_C|^2$ are effective couplings of site "1" with the electrodes.

We need to know the Green function $G_{1,1}^{a,r}$, which is derived by means of the equation-of-motion approach. We get the following set of equations for the single-electron Green functions:

$$\begin{aligned} (\omega - \epsilon_1)G_{1,1}^r &= 1 + t_{01}G_{0,1}^r + t_{12}G_{2,1}^r + UG_{11,1}^r, \\ (\omega - \epsilon_0 + i\Gamma_L + i\Gamma_R)G_{0,1}^r &= t_{01}G_{1,1}^r, \\ (\omega - \epsilon_2 + i\Gamma_C)G_{2,1}^r &= t_{12}G_{1,1}^r. \end{aligned} \quad (9)$$

The equations involve a higher-order Green function $G_{11,1}^r = \langle\langle c_{1\uparrow}c_{1\downarrow}^\dagger | c_{1\uparrow}^\dagger \rangle\rangle_\omega^r$, for which one can write the equation of motion

$$\begin{aligned} (\omega - \epsilon_1 - U)G_{11,1}^r &= n_1/2 + t_{01}(G_{011,1}^r - G_{101,1}^r + G_{110,1}^r) \\ &+ t_{12}(G_{211,1}^r - G_{121,1}^r + G_{112,1}^r), \end{aligned} \quad (10)$$

where n_1 is an average number of electrons accumulated at the QD. All many-particle Green functions are exactly calculated within the three-site system, but the coupling to the electrodes is treated in an approximate way (perturbatively to the order t_a^2)—a similar approximation was used in Refs. 13 and 14. In this approximation we take into account charge fluctuations, but spin-flip processes, which lead to the Kondo resonance, are neglected. In the limit $U \rightarrow \infty$ calculations are simpler and one gets $UG_{11,1}^r \approx -n_1/2$. Therefore, one can calculate from Eq. (9)

$$G_{1,1}^r = (1 - n_1/2)G_{1,1}^{0r}, \quad (11)$$

where $G_{1,1}^{0r}$ is the Green function for noninteracting electrons given by

$$G_{1,1}^{0r} = \frac{1}{\omega - \epsilon_1 - \frac{t_{01}^2}{\omega - \epsilon_0 + i(\Gamma_L + \Gamma_R)} - \frac{t_{12}^2}{\omega - \epsilon_2 + i\Gamma_C}}. \quad (12)$$

(In further considerations we add the superscript "0" to the Green functions corresponding to the system of noninteracting electrons.) Using Eq. (9) one can find all other retarded Green functions: for example,

$$G_{0,0}^r = G_{0,0}^{0r} - \frac{n_1}{2} t_{01}^2 g_0^2 G_{1,1}^{0r}, \quad (13)$$

where $g_0^r = 1/[\omega - \epsilon_0 + i(\Gamma_L + \Gamma_R)]$ and $G_{0,0}^{0r}$ is given by Eq. (5). This result can be used to calculation of the conductance \mathcal{G}_{up} from Eq. (3).

Our approach takes into account the dynamical Coulomb blockade effect. The conductance is expressed by the local Green function $G_{1,1}^r$ [Eq. (11)], which is reduced by the factor $(1 - n_1/2)$ depending on n_1 , the average number of electrons at QD. It is a dynamical process, because an electron at QD blocks for a short time the transmission of other electrons. The Coulomb blockade is known in single-electron sequential transport through quantum dots,³ but this effect is static and charge fluctuations are not allowed (at least for low source-drain voltages).

In order to calculate the conductance \mathcal{G}_{low} we need yet to find the potential V_L in the L electrode treated as the dead wire (i.e., when $J_L = 0$). The current J_L is given by Eq. (2), but it is better to express it by the Green functions $G_{1,1}^{r,a,<}$. Next, one eliminates $G_{1,1}^<$ using Eq. (8) and puts $G_{1,1}^{r,a}$ from Eq. (11). The current

$$J_L = (1 - n_1/2)J_L^0 + \frac{2e}{h} \int_{-\infty}^{\infty} d\omega [f_L(\omega) - f_R(\omega)] 2n_1 \Gamma_L \Gamma_R |g_0|^2, \quad (14)$$

where J_L^0 is the current flowing out from the L electrode calculated using the Green functions for the noninteracting case. From the condition $J_L = 0$ one derives (at $T = 0$) the potential in the left lead

$$V_L = \frac{(1 - n_1/2)|G_{0,0}^0|^2(\Gamma_R V_R + \Gamma_{0C} V_C) + n_1/2|g_0|^2 \Gamma_R V_R}{(1 - n_1/2)|G_{0,0}^0|^2(\Gamma_R + \Gamma_{0C}) + n_1/2|g_0|^2 \Gamma_R}. \quad (15)$$

We work in the quasiequilibrium case, where $V_R = V/2$, $V_C = -V/2$ and the applied potential $V \rightarrow 0$. Now, we can calculate the conductance \mathcal{G}_{low} , which after some algebra is expressed as

$$\mathcal{G}_{low} = \frac{2e^2}{h} 4\Gamma_R \Gamma_{0C} (1 - n_1/2) |G_{0,0}^0|^2 \frac{[(1 - n_1/2)|G_{0,0}^0|^2(\Gamma_L + \Gamma_R + \Gamma_{0C}) + n_1/2|g_0|^2(\Gamma_L + \Gamma_R)]}{(1 - n_1/2)|G_{0,0}^0|^2(\Gamma_R + \Gamma_{0C}) + n_1/2|g_0|^2 \Gamma_R}, \quad (16)$$

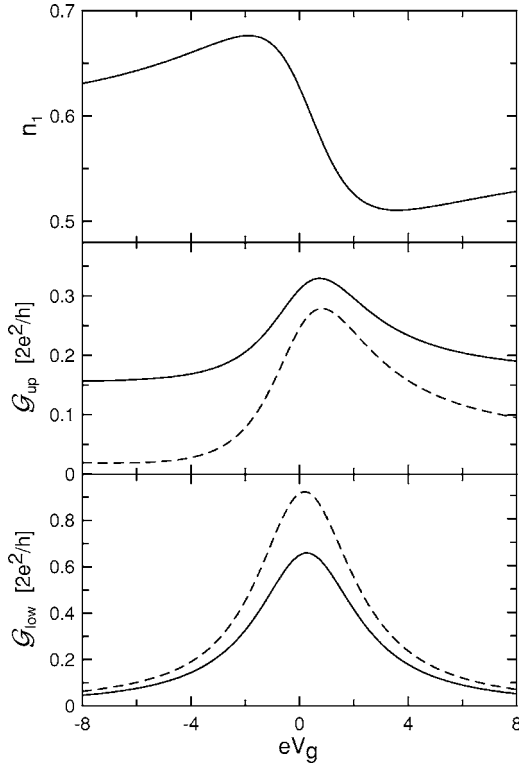


FIG. 3. The number of electrons, n_1 , in the QD (top figure), the conductance \mathcal{G}_{up} (middle figure), and \mathcal{G}_{low} (bottom figure) as a function of the gate voltage V_g for $E_F = -0.25$, $\Gamma_L = 0.16$, $\Gamma_R = \Gamma_C = 1$, $t_{01} = t_{12} = 1$, and $\epsilon_1 = 0$. The dashed curves denote the conductance in the absence of electron-electron interactions.

where all Green functions are taken at E_F . The conductance should be calculated together the number of electrons at QD,

$$n_1 = -i \int \frac{d\omega}{\pi} G_{1,1}^<(\omega), \quad (17)$$

where the lesser Green function is given by Eq. (8).

The results are presented in Fig. 3. The number of electrons at QD decreases, when the central electrode is switched on (for $eV_g > 0$). For this case electrons are more delocalized and can also occupy the junction “2”—leading to reduction n_1 . The conductance \mathcal{G}_{up} is larger than that for the case without electron-electron interactions (compare the solid and dashed curves in Fig. 3). In order to explain this effect we plotted \mathcal{G}_{up} versus the potential ϵ_1 for a QD isolated from the central wire ($t_{12} = 0$)—see Fig. 4. In this case the Fano resonance appears, for which a destructive interference lowers the conductance.⁶ For the noninteracting case the conductance dip is larger and \mathcal{G}_{up} reaches zero at E_F . In the presence of interactions the electron accumulated at QD does not allow traveling waves to penetrate the QD and destructive interference is then less effective.¹² In Fig. 4, \mathcal{G}_{up} is reduced to ca. $1/3 \times 2e^2/h$. If the Kondo resonance is taken into account (in a low-temperature regime), \mathcal{G}_{up} can reach zero,⁷ but it is apart from our approximation.

The conductance \mathcal{G}_{low} is presented in the bottom panel of Fig. 3. Its value is reduced due to interactions (by a factor of ca. 2/3). This is the dynamical Coulomb blockade effect,

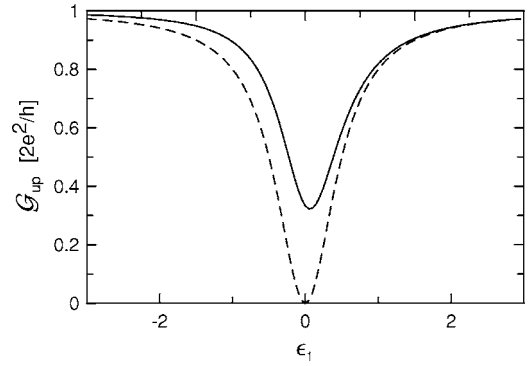


FIG. 4. \mathcal{G}_{up} as a function of the energy level ϵ_1 in the QD, when the central electrode is disconnected ($t_{12} = 0$). The other parameters are $E_F = 0$, $\Gamma_L = \Gamma_R = 1$, and $t_{01} = 1$. The dashed curve is for the free electron system.

because an electron accumulated at QD blocks transfer of another electron. The effect was seen also in the previous paper,¹³ in which the transport through the double-quantum-dot system was studied.

IV. CONCLUDING REMARKS

Summarizing, we have presented electronic transport studies in the three-terminal model, corresponding to the experimental device of two quantum wires coupled through a quantum dot, which was recently investigated by Morimoto *et al.*⁴ The studies have been focused on the influence of resonant transmission from the lower wire on the conductance \mathcal{G}_{up} in the upper wire. The model is simplified and restricted to a single energy level at each junction, and therefore, the conductance \mathcal{G}_{low} shows only a resonant peak instead of quantized plateaus. A more realistic model could have many sites along and across the quantum point contact; it could include changes of the height and width of the barrier potential with applied gate potential. For this case one could expect many conductance plateaus with a pronounced resonant peak in front of each step. However, the experiment⁴ showed that changes in \mathcal{G}_{up} are evidently due to a resonant channel and our simplification is justified.

The experiment of Morimoto *et al.*⁴ was for first time analyzed theoretically by Puller *et al.*⁵ Their model is a two-terminal system connected to a QD. The calculations⁵ were done in a single-electron approximation [the electron-electron interactions were treated in the Hartree-Fock (HF) approximation]. Our calculations go beyond the HF approximation, and two-particle Green functions are taken into account. Therefore, the present procedure includes a dynamical Coulomb blockade effect, although it neglects spin-flip processes and the Kondo resonance. Puller *et al.*⁵ also included interference waves penetrating the QD and a dip in the conductance was seen, but the calculations were restricted to the second order of the wire-QD coupling (to t_{01}^2 in our notation). Our procedure takes into account all scattering on the QD as well on the contacts, and therefore, the Fano resonance can be observed.

The measurements by Morimoto *et al.*⁴ showed a sharp resonantlike peak, without any features of destructive inter-

ference. In our studies a peak in \mathcal{G}_{up} can be observed with small asymmetry if the position of the Fermi energy E_F is close to the QD state ϵ_1 (in our notation $E_F \approx 0$). The experiment⁴ also showed that the QD plays a minor role in the interwire coupling. They repeated the transport measurements grounding one of the gates close to QD. The interwire coupling was then through a very large quantum dot. They observed essentially the same resonance effect. Although additional coupling channels were opened, they did not change the conductance. In our model we have increased the QD coupling t_{01} and t_{12} by an order of magnitude (from 1 to 10), but for small E_F the conductance \mathcal{G}_{up} has been only slightly affected. The peak in the conductance was also observed experimentally for multichannel transport,⁴ when the quantum point contact in the upper wire was broad enough to

allow transmission of many electronic waves. The relative height of the peak slightly increased (in the range $0.05-0.08 \times 2e^2/h$) with increasing number of channels. It may suggest that the resonant transmission from the lower wire is coupled with the edge states and higher transmission channels are not affected.

ACKNOWLEDGMENTS

The work was supported by the project RTNNANO Contract No. MRTN-CT-2003-504574, in part (B.R.B.) by the Ministry of Science and Higher Education (Poland), and in part (M.T. and I.V.D.) by Romanian Excellence Program No. CEEX-D11-45.

¹C. C. Eugster and J. A. del Alamo, Phys. Rev. Lett. **67**, 3586 (1991); C. C. Eugster, J. A. del Alamo, M. J. Rooks, and M. R. Melloch, Appl. Phys. Lett. **60**, 642 (1992); C. C. Eugster, J. A. del Alamo, M. R. Melloch, and M. J. Rooks, Phys. Rev. B **48**, 15057 (1993); J. A. del Alamo and C. C. Eugster, Jpn. J. Appl. Phys., Part 1 **34**, 4439 (1995).

²A. Bertoni, P. Bordone, R. Brunetti, C. Jacoboni, and S. Reggiani, Phys. Rev. Lett. **84**, 5912 (2000).

³D. K. Ferry and S. M. Goodnick, *Transport in Nanostructures* (Cambridge University Press, Cambridge England, 1997).

⁴T. Morimoto, Y. Iwase, N. Aoki, T. Sasaki, Y. Ochiai, A. Shailos, J. P. Bird, M. P. Lilly, J. L. Reno, and J. A. Simmons, Appl. Phys. Lett. **82**, 3952 (2003); see also J. P. Bird and Y. Ochiai, Science **303**, 1621 (2004); A. Shailos, Y. Ochiai, T. Morimoto, Y. Iwase, N. Aoki, T. Sasaki, J. P. Bird, M. P. Lilly, J. L. Reno, and J. A. Simmons, Semicond. Sci. Technol. **19**, S405 (2004).

⁵V. I. Puller, L. G. Mourokh, A. Shailos, and J. P. Bird, Phys. Rev.

Lett. **92**, 096802 (2004).

⁶See, for example, H. Xu and W. Sheng, Phys. Rev. B **57**, 11903 (1998); K. Kang, S. Y. Cho, and J. J. Kim, *ibid.* **65**, 153303 (2002).

⁷P. Stefanski, Solid State Commun. **128**, 29 (2003); I. Maruyama, N. Shibata, and K. Ueda, J. Phys. Soc. Jpn. **73**, 3239 (2004).

⁸M. Sato, H. Aikawa, K. Kobayashi, S. Katsumoto, and Y. Iye, Phys. Rev. Lett. **95**, 066801 (2005).

⁹H. Haug and A.-P. Jauho, *Quantum Kinetics in Transport and Optics of Semiconductors* (Springer-Verlag, Berlin, 1998).

¹⁰M. Buttiker, Phys. Rev. Lett. **57**, 1761 (1986); H. Q. Xu, Appl. Phys. Lett. **78**, 2064 (2001); see also Ref. 3.

¹¹U. Fano, Phys. Rev. **124**, 1866 (1961).

¹²P. Stefanski, A. Tagliacozzo, and B. R. Bulka, Phys. Rev. Lett. **93**, 186805 (2004).

¹³B. R. Bulka and T. Kostyrko, Phys. Rev. B **70**, 205333 (2004).

¹⁴T. Kostyrko and B. R. Bulka, Phys. Rev. B **71**, 235306 (2005).